International Journal of Nanomedicine

Dovepress
Taylor & Francis Group

Open Access Full Text Article

ORIGINAL RESEARCH

MiR-148a-3p Loaded Human Umbilical Cord Mesenchymal Stem Cell-Derived Extracellular Vesicles Alleviates Silica-Induced Pulmonary Fibrosis by Inhibiting β-Catenin Signaling

Qiyue Jiang[1,2], Fuao Ning[1,2], Qiyue Jia[1,2], Hongwei Wang[1,2], Wenming Xue[1,2], Jiaxin Wang[1,2], Yan Wang[1,2], Zhonghui Zhu[1,2], Lin Tian[1,2]

[1]Department of Occupational and Environmental Health, School of Public Health, Capital Medical University, Beijing, 100069, People's Republic of China; [2]Beijing Key Laboratory of Environment and Aging, Capital Medical University, Beijing, 100069, People's Republic of China

Correspondence: Lin Tian; Zhonghui Zhu, Department of Occupational and Environmental Health, School of Public Health, Capital Medical University, Beijing, 100069, People's Republic of China, Email tian_lin@163.com; zhuzhonghui@163.com

Background: In clinical practice, due to the lack of typical symptoms and specific diagnostic biomarkers, silicotic patients often having already developed pulmonary fibrosis by the time of clinical diagnosis. Studies have demonstrated that human umbilical cord mesenchymal stem cell-derived extracellular vesicles (hucMSC-EVs) could moderate silicosis fibrosis, which may be related to the microRNAs (miRNAs) in hucMSC-EVs. While the full extent of their antifibrotic effects and the underlying mechanisms remain to be elucidated.

Methods: HucMSC-EVs were administered from day 28 to day 56 after silica exposure in mice, which in a therapeutic manner. In addition, the antifibrotic abilities of engineered hucMSC-EVs with varying levels of miR-148a-3p, a miRNA with antifibrotic properties, were evaluated. Heat shock protein 90 beta family member 1 (Hsp90b1) is reported to be a target of miR-148a-3p, the protein-protein interaction analysis was used to explore its regulated downstream factors in lung fibrosis. The underlying mechanisms were also investigated by using miR-148a-3p mimics and small interfering RNA (siRNA) targeting Hsp90b1 in vitro.

Results: HucMSC-EVs could reduce the histopathological changes and the levels of fibrotic proteins in the mouse lung tissues when administered in a therapeutic manner. Meanwhile, miR-148a-3p-overexpressed hucMSC-EVs intervention exhibited the enhanced anti-fibrotic effect compared with the negative control intervention group. In vitro, the elevated level of miR-148a-3p in hucMSC-EVs was shown to enhance hucMSC-EVs' inhibition of fibroblast collagen hypersecretion, whereas a depressed level of miR-148a-3p in hucMSC-EVs partially counteracted the inhibitory effect. Moreover, the mechanistic investigations revealed that miR-148a-3p could blunt β-catenin signaling via targeting Hsp90b1 in fibroblasts.

Conclusion: This study demonstrated that hucMSC-EVs retain their antifibrotic properties in silicotic mice when administered in a therapeutic manner. Further, miR-148a-3p was confirmed to be an essential component within hucMSC-EVs, mediating their inhibition of silica-induced pulmonary fibrosis by reducing β-catenin signaling via targeting of Hsp90b1 in fibroblasts.

Plain Language Summary: Silicosis is a life-threatening occupational pulmonary fibrotic disease caused by silica inhalation, and there is currently a lack of targeted drugs for treating silicosis. Extracellular vesicles (EVs) are emerging as pivotal players in cell-free therapeutics due to their crucial role in intercellular communication and the efficient transport of bioactive molecules. In this study, the antifibrotic effects of human umbilical cord mesenchymal stem cell-derived EVs (hucMSC-EVs) on experimental silicosis were investigated. HucMSC-EVs were administered therapeutically, an approach that aligns more closely with the clinical situation of silicosis. In addition, the antifibrotic abilities of engineered hucMSC-EVs with varying levels of miR-148a-3p, a microRNA (miRNA) with antifibrotic properties, were evaluated. The underlying mechanisms that contribute to these therapeutic effects were also investigated. The results demonstrated that hucMSC-EVs retain their antifibrotic properties in silicotic mice when administered in a therapeutic manner. Further, miR-148a-3p was confirmed to be an essential component within hucMSC-EVs, mediating their inhibition of silica-induced pulmonary fibrosis by reducing β-catenin signaling via targeting of heat shock protein 90 beta family

Received: 26 November 2024
Accepted: 11 March 2025
Published: 9 April 2025

member 1 (Hsp90b1) in fibroblasts. These insights provide strong empirical support for hucMSC-EVs-based therapy as a novel treatment approach for silicosis and other lung fibrotic diseases.

Keywords: MiR-148a-3p, extracellular vesicles, pulmonary fibrosis, β-catenin, Hsp90b1, silica

Graphical Abstract

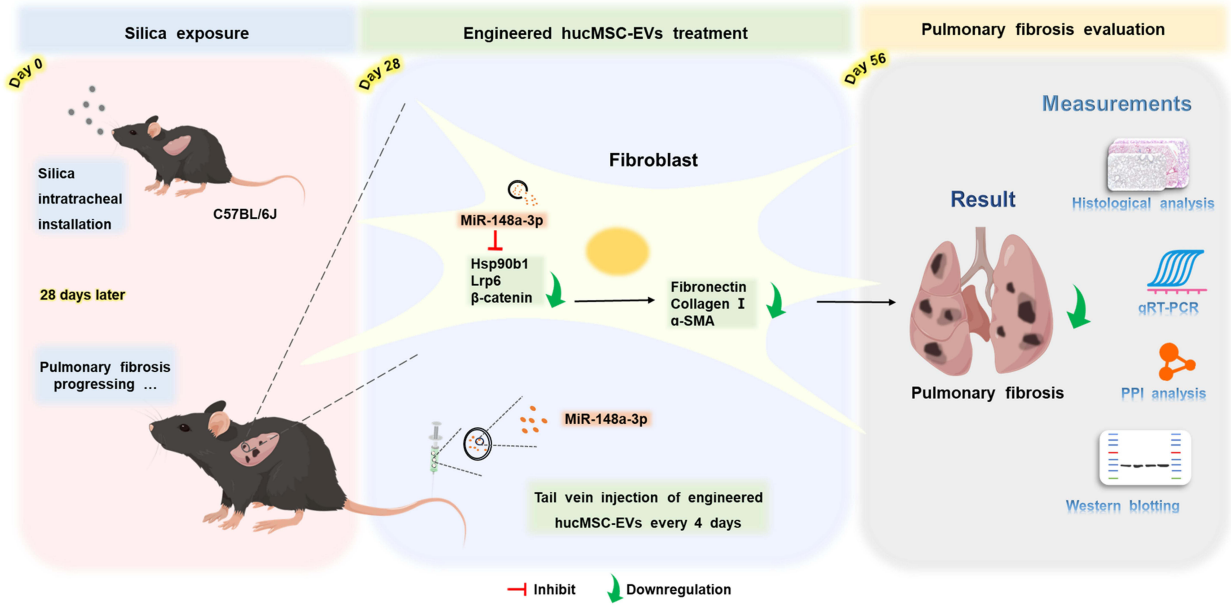

Introduction

Extracellular vesicles (EVs) are nano- to micro-sized particles with a bilayer lipid membrane structure that appear to be released by all cell types into the surrounding environment.[1] In recent years, EVs have attracted the attention of many researchers, particularly in the fields of cell-free therapy and drug delivery systems, due to their prominent roles in intercellular communication and material transportation.[2] For cell-free therapy, EVs can mimic and manifest the damage repair ability of their parental cells while avoiding the risks of embolization or tumorigenicity associated with cell therapy.[3] For drug delivery, the bilayer lipid membrane of EVs provides an exceptional protective barrier for their contents, ensuring stability and potentially offering superior safety profiles compared to conventional carriers such as liposomes or nanoparticles.[4] Thus, EVs are emerging as pivotal plays in the biomedical field.

Silicosis is a life-threatening occupational pulmonary fibrotic disease caused by silica inhalation. It is characterized by excessive deposition of extracellular matrix (ECM) proteins (including Collagen I, Fibronectin, etc.) in the lung interstitium, replacing normal lung tissue, and the formation of silicon nodules.[5] At present, the pathogenesis of silicosis is not completely understood. When activated by a range of pro-fibrotic factors, with transforming growth factor-β1 (TGF-β1) being the most influential, resting fibroblasts undergo a transformation characterized by elevated expression of α-smooth muscle actin (α-SMA) and a hypersecretory phenotype of ECM proteins, also known as myofibroblasts, which are pivotal to the progression of fibrosis in silicosis.[6] In clinical practice, the lack of typical symptoms and specific diagnostic biomarkers, and the delayed diagnosis of silicosis, with patients often having already developed pulmonary fibrosis by the time of clinical diagnosis, pose a great challenge to the treatment of silicosis.[7] Therefore, preclinical

experimental studies utilizing silicotic models with established pulmonary fibrosis offer more relevance and are close to the clinical reality of silicosis patients.[8]

The therapeutic options for silicosis remain limited. Lung transplantation, the primary option for severe cases, is limited by its high costs, complex surgery, and donor shortages. Fortunately, basic research on the treatment of silicosis has yielded encouraging results. Pirfenidone and Nintedanib, which are approved for idiopathic pulmonary fibrosis have also shown an anti-fibrotic effect in silicotic models.[8–10] Additionally, mesenchymal stem cells (MSCs) have recently emerged as cellular therapeutic agents for silicosis due to their powerful multi-effect repair ability.[11–13] Studies have demonstrated that EVs derived from MSCs (MSC-EVs) inherit the anti-fibrotic function of their parental cells, and contents encapsulated in MSC-EVs are known to partially mediate their anti-fibrotic function.[14,15] Despite the demonstrated potential of MSC-EVs in experimental silicosis models, the full extent of their antifibrotic effects and the underlying mechanisms remain to be elucidated.

Studies are increasingly demonstrating that microRNAs (miRNAs) are integral to the functionality of EVs as key components of the molecular cargo they transport.[16,17] MiRNAs are small and short non-coding RNAs that play pivotal roles in a myriad of biological processes by binding to the complementary sequences of target mRNAs.[18] Previous research has demonstrated that miR-148a-3p, a miRNA with antifibrotic properties that is enriched in human umbilical cord MSC-EVs (hucMSC-EVs), plays a role in the prevention of experimental silicosis by directly targeting heat shock protein 90 beta family member 1 (Hsp90b1), thereby suppressing fibroblast collagen secretion.[19] Nevertheless, the exact function of miR-148a-3p in hucMSC-EVs and the mechanisms involving Hsp90b1 regulation remain to be elucidated.

The β-catenin signaling pathway, a pathway that plays an important role in modulating cell differentiation, proliferation, and migration, is abnormally activated in fibrotic lung diseases, particularly in silicosis.[20,21] It has demonstrated that Grp94, the protein Hsp90b1 encodes, can regulate β-catenin signaling by controlling the expression of low-density lipoprotein receptor-related protein 6 (Lrp6) in intestinal disease.[22–24] However, few reports have detailed the association between Hsp90b1 and β-catenin signaling in silicosis, and there is a lack of studies exploring the link between β-catenin signaling and the mitigation of silica-induced fibrotic pulmonary disease by hucMSC-EVs, including the potential underlying mechanisms.

Thus, the aim of this study was to explore whether hucMSC-EVs retain antifibrotic effects in silicotic mice when administered in a therapeutic manner. Further, hucMSC-EVs with varying levels of miR-148a-3p were engineered and the specific role of miR-148a-3p in mitigating silicosis was investigated in an experimental model. Finally, the roles of miR-148a-3p's target Hsp90b1 and the β-catenin signaling pathway were investigated in fibroblasts.

Materials and Methods

Engineered hucMSC-EVs

MiR-148a-3p-overexpressed lentivirus vector [virus miR-148a-3p (+)]/negative control lentivirus vector (virus NC) (Genechem Inc, Shanghai, China), miR-148a-3p mimics/mimics NC, and miR-148a-3p inhibitor/inhibitor NC (Sangong Biotech Co., Ltd., Shanghai, China) were respectively transfected into hucMSCs (NUWACELL Co., Ltd. Anhui, China). The culture medium was collected for centrifugation, filtration, concentration, and re-centrifugation to obtain the corresponding engineered hucMSC-EVs with different levels of miR-148a-3p. The exact method of engineering hucMSC-EVs has been previously described in detail.[19] The sequences are shown in Supplementary Table S1.

In Vivo Tracking

Specific pathogen-free (SPF) C57BL/6J (male, weight 20–22 g) mice were obtained from Vital River Laboratory Animal Technology (Beijing, China). The mice were intravenously administered fluorescent 1.1′-dioctadecyl-3,3,3′,3′-tetramethylindotricarbocyanine iodide (DiR) (D12731, Thermo Fisher Scientific, OR, USA)-labeled EVs-virus miR-148a-3p (+), with approximately 200 μg of protein resuspended in 100 μL of saline. Injection of 100 μL of saline served as the control. At selected time points after administration, the mice were anesthetized and euthanized. Then, the lung tissues were collected and imaged 24 h, 48 h, 72 h, 96 h, and 120 h post-administration. An IVIS Spectrum imaging system (PerkinElmer, MA, USA) was used to capture the fluorescent signal. DiR: excitation = 745 nm; emission = 800 nm.

Additionally, the mice were intravenously administered PKH26 (UR52302, Umibio Co., Ltd., Shanghai, China)-labeled EVs-virus miR-148a-3p (+), with approximately 200 μg of protein resuspended in 100 μL of saline. At 48 hours after administration, the mice were anesthetized and euthanized. Then, the lung tissues were collected and embedded in OTC for frozen sectioning at 10 μm. Subsequently, immunofluorescence staining of the frozen sections was performed to further localize the EVs-virus miR-148a-3p (+) in the mouse lung tissues. PKH26: excitation = 551 nm; emission = 567 nm.

Establishment of the Silicotic Mouse Model

The engineered hucMSC-EVs obtained by lentivirus vector transfection were used for in vivo experiments; these were named EVs-virus miR-148a-3p (+) and EVs-virus NC. C57BL/6J mice (SPF, male, weight 20–22 g) were randomly divided into five groups: control, silica, silica + hucMSC-EVs, silica + EVs-virus NC, and silica + EVs-virus miR-148a-3p (+), with n=10 per group. The silicotic mouse model was generated via intratracheal instillation of 2.5 mg of silica (Sigma, MO, USA) in 50 μL of saline. The control group received 50 μL of saline. HucMSC-EVs, EVs-virus NC, and EVs-virus miR-148a-3p (+) (200 μg/100 μL) were injected via tail vein every 4 days from day 28 post-silica instillation; 100 μL of saline was injected into the other two groups mice. On the 56th day after silica instillation, the mice were anesthetized and sacrificed to collect lung tissues for examination.

Hydroxyproline Assay

The hydroxyproline (HYP) concentrations in the lung tissues of the mice were detected using a HYP colorimetric assay kit (A303-2-1, Nanjing Jiancheng Bioengineering Institute Co., Ltd., Nanjing, China). The absorbance at 550 nm was measured by a microplate reader (Bio-Tek EPOCH2) and then converted to the HYP concentration (μg/mg).

Histopathological and Immunohistochemical Assessments

The lung tissues of mice were prepared into paraffin sections (approximately 5 μm thick). Hematoxylin and Eosin (HE) and Masson staining were used to assess structural changes and collagen deposition in the lung tissue samples. The α-SMA, Grp94, and β-catenin proteins in the lung tissues were detected by immunohistochemical (IHC) staining. An Aperio ImageScope (Leica Biosystems Imaging, Inc., CA, USA) was used to acquire representative images. The antibodies used are available in Supplementary Table S2.

NIH/3T3 Cell Treatment

The engineered hucMSC-EVs obtained by miR-148a-3p mimics/mimics NC and miR-148a-3p inhibitor/inhibitor NC transfection were used for in vitro experiments; these were defined as EVs-miR-148a-3p (+/-) and corresponding EVs-NC. A hypersecretory phenotype of fibroblasts was induced with NIH/3T3 cells (murine fibroblast cell line), which were obtained from the Cell Resource Center, Peking Union Medical College (PCRC) (Beijing, China), stimulated by 5 ng/mL TGF-β1 (PeproTech, NJ, USA), and simultaneously engineered hucMSC-EVs were administered at 50 μg/mL. Transfection of MiR-148a-3p mimics and small interfering RNA (siRNA) targeting Hsp90b1 (siHsp90b1) (Sangong Biotech Co., Ltd., Shanghai, China) was performed as described in the Supplementary Methods.

RNA Isolation and Quantitative Real-Time PCR (qRT-PCR) Analysis

The total RNA was extracted via TRIzol reagent (Thermo Fisher Scientific, USA) and then the total RNA was reverse transcribed into cDNA using TransScript miRNA First Strand cDNA Synthesis SuperMix (AT351, TransGen Biotech, Beijing, China). qRT-PCR was amplified with PerfectStart Green qPCR SuperMix (AQ601, TransGen Biotech, Beijing, China) using a CFX96 RT-qPCR detection system (Bio-Rad, CA, USA). The relative expression levels of the groups were calculated using the $2^{-\Delta\Delta Ct}$ method. The primer sequences are available in Supplementary Table S3.

Western Blotting Analysis

The total proteins were extracted from the lung tissues and cells using radioimmunoprecipitation (RIPA) lysis buffer (Beyotime Biotechnology, Shanghai, China). A Nuclear and Cytoplasmic Protein Extraction Kit (P0028, Beyotime

Biotechnology, Shanghai, China) was used to extract the nuclear and cytoplasmic protein of NIH/3T3 cells. The extracted protein samples (20–40 μg) were separated on SDS-PAGE and transferred onto PVDF membranes (Millipore, MA, USA). They were then incubated overnight at 4°C with primary antibodies and the corresponding secondary antibody. ECL Detection Reagent (NCM Biotech, Suzhou, China) was used to visualize the proteins with a Tanon-5200 system (Beijing Yuan Ping Hao Biotech, Shanghai, China). The densities of the bands were quantified using Image J software. The antibodies used for these analyses are described in Supplementary Table S4.

Immunofluorescence

NIH/3T3 cells were rinsed, fixed, permeabilized, blocked, and incubated with the β-catenin antibody at 4°C overnight. The cells were then incubated with the fluorescent-labeled secondary antibody [anti-rabbit IgG (H + L)] at room temperature for 1 h, and then the nuclei were stained with DAPI (ZLI-9557, ZSGB-BIO, Beijing, China). Laser-scanning confocal fluorescence microscopy (ECLIPSE Ti2, Nikon, Japan) was used to obtain images.

The frozen slices of lung tissue were blocked in 5% goat serum for 1 h and incubated with the α-SMA antibody at 4°C overnight. The slices were then incubated with fluorescent-labeled secondary antibody [anti-mouse IgG (H + L)] at room temperature for 1 h, and the nuclei were stained with DAPI for fluorescent signal analysis.

The antibodies used in these analyses are described in Supplementary Table S5.

Statistical Analysis

The data were analyzed using SPSS 24.0 and visualized with GraphPad Prism 8.0. Student's t-tests or one-way ANOVA were used to examine statistical differences between the groups. All experiments were performed independently at least three times. Data are presented as the mean ± standard deviation (SD) and statistical significance was set at $p < 0.05$.

Further detail on the methods and analyses can be found in the Supplementary Information.

Results

Therapeutic Administration of hucMSC-EVs Ameliorates Silica-Induced Pulmonary Fibrosis in Mice

Our previous study indicated that lung tissue undergoes fibrosis on day 28 after exposure to silica suspension.[25] To explore whether hucMSC-EVs maintain antifibrotic effects in silicotic mice when administered in a therapeutic manner, mice were given tail vein injections of hucMSC-EVs starting from day 28 to day 56 post-silica instillation, using the same modeling method as our previous study (Figure 1A). This regimen was designated as therapeutic administration, in contrast to the prophylactic administration protocol adopted in our previous studies, where hucMSC-EVs were injected on the first day following silica exposure.[26] The hucMSC-EVs intervention significantly attenuated silica-induced pulmonary injury, as demonstrated by the HE and Masson staining results (Figure 1B). The lung tissues of mice in the silica group showed a loss of normal alveolar structure, characterized by thickened alveolar walls and collapsed alveoli. Moreover, significant cellular infiltration was observed in the lung interstitium, resulting in the formation of cell clusters or nodules, alongside extensive deposition of blue-stained collagen. However, treatment with hucMSC-EVs alleviated these abnormalities, although some pathological changes in the fibrotic lung tissue structures persisted. Consistently, the HYP assay showed that the hucMSC-EVs intervention downregulated the collagen content compared with that of the silica group (Figure 1C). The expression levels of fibrotic proteins (Fibronectin, Collagen I, and α-SMA) were increased in silicotic lungs, and were obviously diminished by the hucMSC-EVs intervention (Figures 1D-E). IHC analysis also showed α-SMA expression in the fibrotic areas of the lung tissue, consistent with the findings of the Western blotting analysis (Figure 1F and Figure S1A). The above results indicate that hucMSC-EVs exerted anti-fibrotic effects in the silicotic mouse model which is characterized by pulmonary fibrosis. This suggests that hucMSC-EVs retain antifibrotic effects in silicotic mice under therapeutic administration, although it could not completely reverse pulmonary fibrosis.

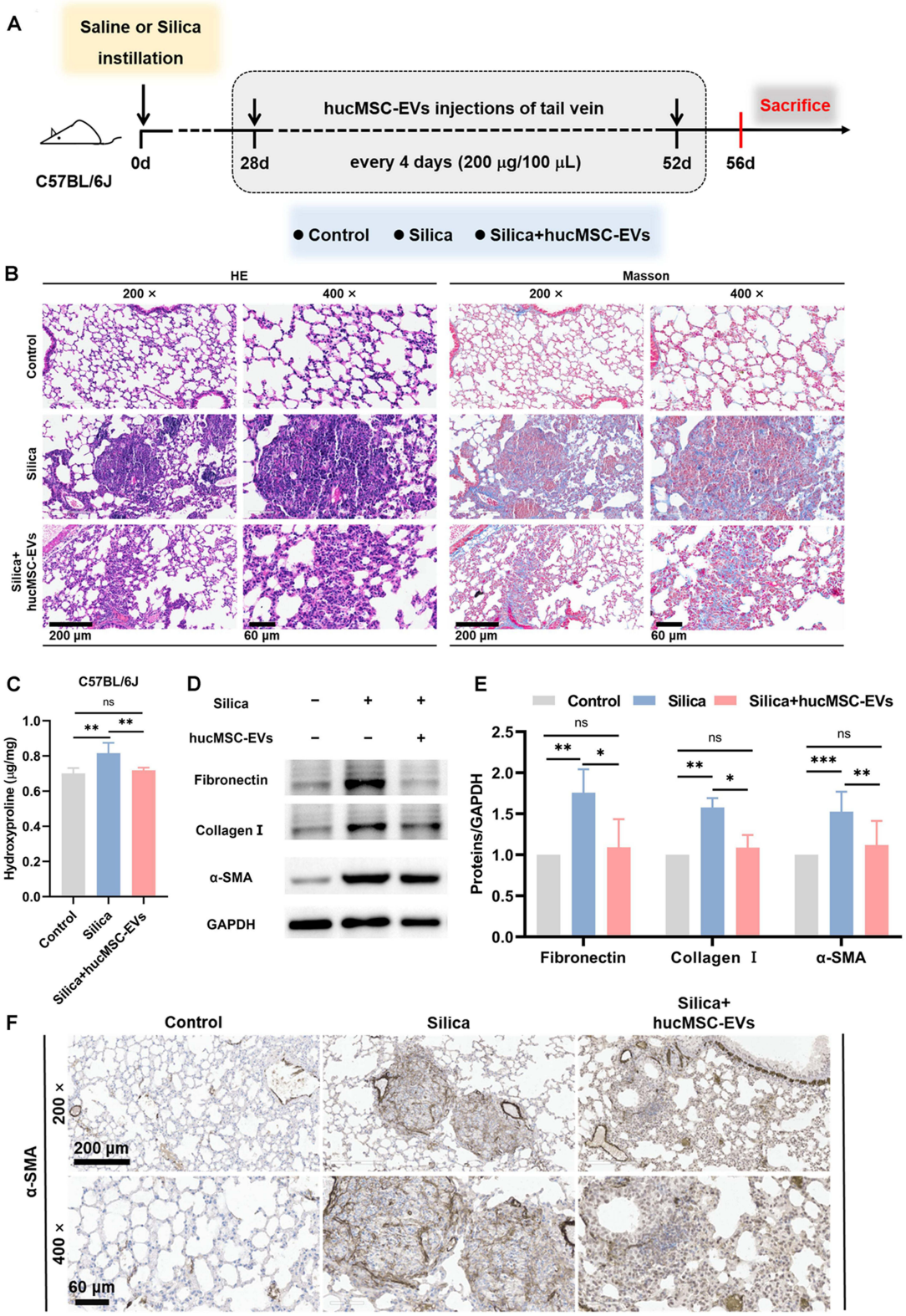

Figure 1 Therapeutic administration of hucMSC-EVs ameliorates silica-induced pulmonary fibrosis in mice. (**A**) Schematic of the study design and modeling. (**B**) HE and Masson staining of lung sections (200 ×, bar: 200 μm and 400 ×, bar: 60 μm). (**C**) The content of HYP (n = 3–4). (**D-E**) Fibronectin, Collagen I, and α-SMA protein levels in mice lung tissues (n = 3–7). (**F**) IHC staining of α-SMA in mice lung tissues (200 ×, bar: 200 μm and 400 ×, bar: 60 μm). ns $p > 0.05$, *$p < 0.05$, **$p < 0.01$, ***$p < 0.001$ (One-way ANOVA). Data are presented as the means ± SD.

 https://doi.org/10.2147/IJN.S506542

MiR-148a-3p Plays an Active Role in the Alleviation of Lung Fibrosis in Silicotic Mice by hucMSC-EVs

To explore the critical role of miR-148a-3p in the hucMSC-EVs intervention, miR-148a-3p-overexpressed lentivirus vector [virus miR-148a-3p (+)] was used to generate miR-148a-3p-overexpressed hucMSCs, from which, miR-148a-3p-overexpressed hucMSC-EVs [EVs-virus miR-148a-3p (+)] were subsequently obtained. Figure 2A and B show that transfection with virus miR-148a-3p (+) significantly upregulated the level of miR-148a-3p in hucMSCs and their derived EVs compared with the negative control lentivirus vector (virus NC) treatment. The isolation and characterization of hucMSC-EVs were conducted as previously described.[19]

To verify if EVs-virus miR-148a-3p (+) reached the lungs, DiR-labeled EVs-virus miR-148a-3p (+) was intravenously given to mice through the tail vein, and lung fluorescence at various time points was observed. Bioluminescence imaging (Figure 2C) showed that 72 h post-injection was a critical time point, with the lung fluorescence intensifying

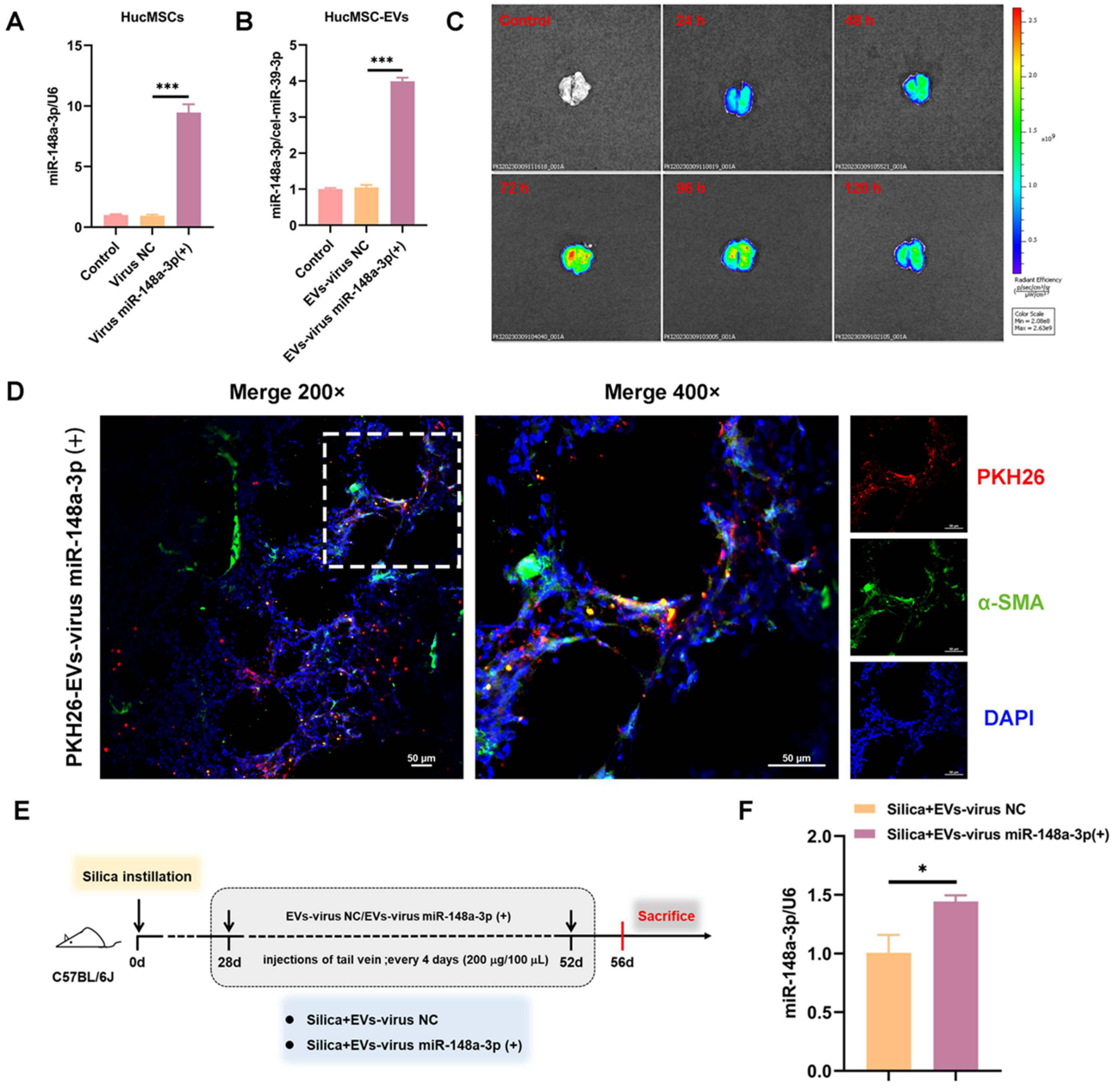

Figure 2 Continued.

https://doi.org/10.2147/IJN.S506542

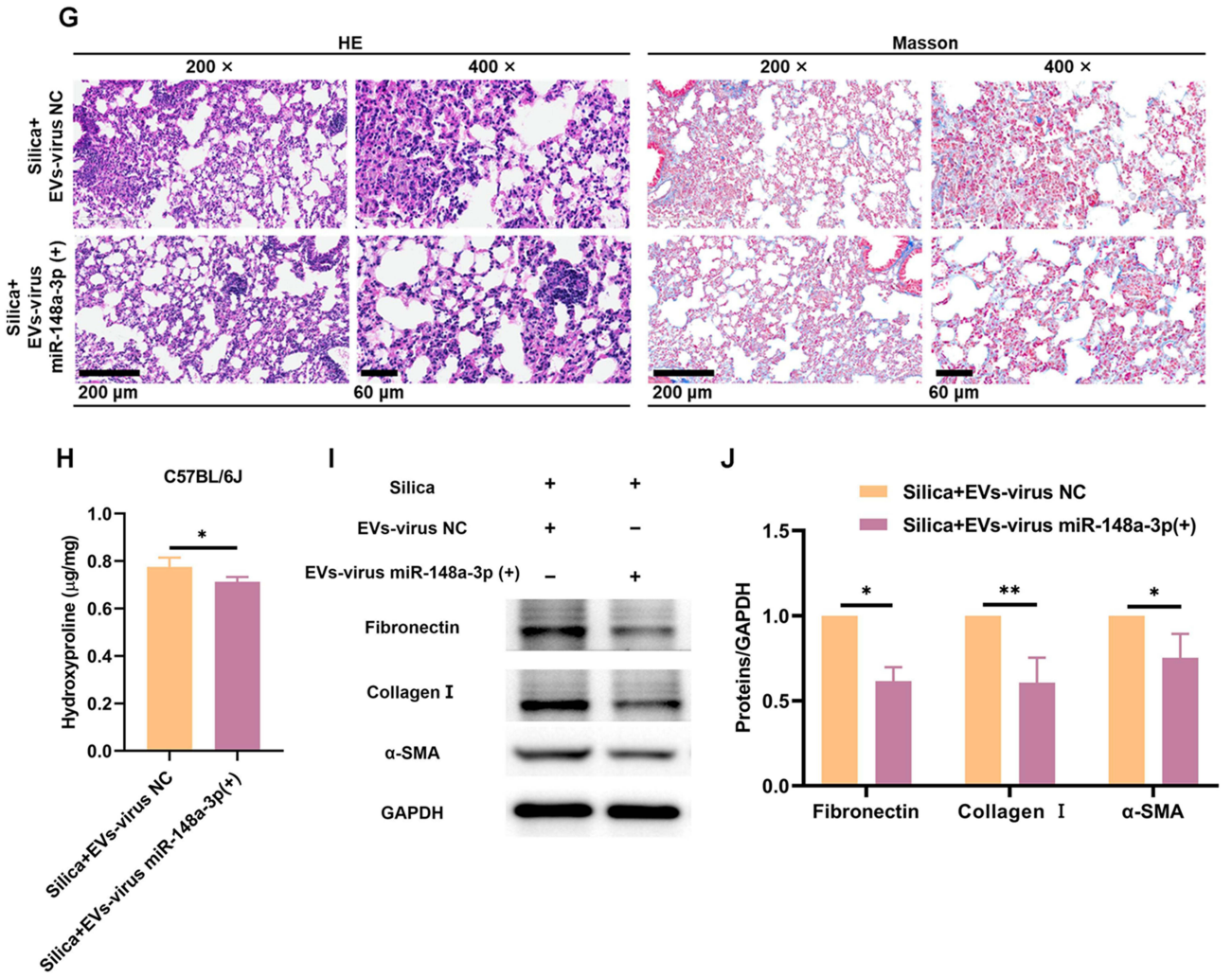

Figure 2 MiR-148a-3p plays an active role in the alleviation of lung fibrosis in silicotic mice by hucMSC-EVs. (**A**) MiR-148a-3p level in hucMSCs transfected with lentivirus vector of miR-148a-3p-overexpression/negative control (NC) (n = 6). (**B**) MiR-148a-3p level in hucMSC-EVs obtained from hucMSCs with different treatments (n = 3). (**C**) Tracking of DiR-labeled miR-148a-3p-overexpressed hucMSC-EVs in mice lung tissues at different time points (24 h, 48 h, 72 h, 96 h, and 120 h) by IVIS Spectrum imaging system (DiR: excitation = 745 nm; emission = 800 nm). (**D**) Representative images showing the α-SMA (green) of mice lung tissues frozen slices after treatment with PKH26-labeled EVs-virus miR-148a-3p (+) (red) (PKH26: excitation = 551 nm; emission = 567 nm; Bar: 50 μm). (**E**) Schematic of the study design and modeling. (**F**) The level of miR-148a-3p in mice lung tissues (n = 3). (**G**) HE and Masson staining of lung sections (200 ×, bar: 200 μm and 400 ×, bar: 60 μm). (**H**) The content of HYP (n = 3–4). (**I-J**) Fibronectin, Collagen I, and α-SMA protein levels in mice lung tissues (n = 3–7). *$p < 0.05$, **$p < 0.01$, ***$p < 0.001$ (One-way ANOVA was used to compare between multiple groups and Student's t-tests was used to compare between two groups). Data are presented as the means ± SD.

until reaching a peak at 72 h and subsequently diminishing. The fluorescence intensity remained a high level at 96 h, with signals persisting in the lungs up to 120 h post-injection. This suggests that administering these EVs every 96 h (4 days) could maintain their presence in vivo. Additionally, immunofluorescent staining was performed to determine the binding affinity of EVs-virus miR-148a-3p (+) to myofibroblasts, the pivotal effector cells in the progression of silicosis, which could be derived from lung fibroblasts and is characterized by elevated expression of α-SMA. Mice were injected with PKH26-labeled EVs-virus miR-148a-3p (+), and lung tissues were harvested and prepared into frozen sections 48 h later. Immunofluorescent staining of the section was then performed using α-SMA. The immunofluorescence assay demonstrated co-localization of α-SMA (green) and PKH26 (red) fluorescent signals within the lung interstitium, confirming the binding capability of EVs-virus miR-148a-3p (+) to these cells (Figure 2D). Thus, these findings suggest that EVs-virus miR-148a-3p (+) successfully reached the lung tissue and may be able to bind to lung myofibroblasts.

Subsequently, EVs-virus miR-148a-3p (+) and its negative control EVs-virus NC were administrated to mice every 4 days under the therapeutic administration protocol (Figure 2E). The results showed that the miR-148a-3p level was higher in the lungs of the silica + EVs-virus miR-148a-3p (+) group than in the group treated with EVs-virus NC

(Figure 2F). This suggests that EVs-virus miR-148a-3p (+) effectively increased the miR-148a-3p level in silicotic mice lung tissues. Furthermore, the lung histopathologic changes (Figure 2G), HYP content (Figure 2H), and the expression levels of fibrotic proteins in the lung tissues (Figures 2I-J) were reduced in the silica + EVs-virus miR-148a-3p (+) group as compared to the silica + EVs-virus NC group. This suggests that the increased miR-148a-3p content further amplified the antagonistic fibrosis effect of hucMSC-EVs, as compared with the EVs-virus NC intervention, indicating that miR-148a-3p plays an active role in the alleviation of lung fibrosis in silicotic mice by hucMSC-EVs.

In Vitro Validation of the Function of miR-148a-3p in hucMSC-EVs

To further determine the function of miR-148a-3p in hucMSC-EVs, the hucMSC-EVs containing varying levels of miR-148a-3p was applied to TGF-β1-treated NIH/3T3 cells. TGF-β1, known as a potent pro-fibrotic factor, is commonly used to induce a fibroblast hypersecretory phenotype. Figure 3A and C show that compared with EVs isolated from the corresponding NC-transfected hucMSCs (EVs-NC), miR-148a-3p expression was higher in EVs-miR-148a-3p (+) and lower in EVs-miR-148a-3p (-). This confirms the successful preparation of the desired hucMSC-EVs. The in vitro tracking results showed that five types of hucMSC-EVs [hucMSC-EVs, EVs-miR-148a-3p (+/-), and the corresponding EVs-NC] were taken up by NIH/3T3 cells (Figure S2). Subsequently, the hucMSC-EVs interventions were found to significantly upregulate miR-148a-3p expression in NIH/3T3 cells compared with the TGF-β1 group, with levels being higher after EVs-miR-148a-3p (+) treatment and lower in the EVs-miR-148a-3p (-) treatment group versus the EVs-NC treatment (Figure 3B and D). Next, the levels of fibrosis-related proteins were assessed in NIH/3T3 cells. Western blotting analysis demonstrated increased levels of these proteins in the TGF-β1 group, which were reduced following hucMSC-EVs treatment. Notably, the EVs-miR-148a-3p (+) treatment more effectively reduced these protein levels compared to the EVs-NC treatment (Figure 3E and G). These findings indicate that the upregulation of miR-148a-3p in hucMSC-EVs bolstered their inhibitory impact on TGF-β1-induced collagen hypersecretion of fibroblasts. Furthermore, the downregulation of miR-148a-3p could blunt the beneficial function of hucMSC-EVs against TGF-β1-induced collagen hypersecretion of fibroblasts (Figure 3F and H). These observations collectively highlight the pivotal role of miR-148a-3p in mediating the inhibitory effect of hucMSC-EVs on the TGF-β1-induced hypersecretory phenotype of fibroblasts.

β-Catenin Signaling Is Implicated in the Anti-Fibrotic Effect of miR-148a-3p-Mediated hucMSC-EVs in Silicotic Mice Pulmonary Fibrosis

Next, the potential mechanism by which miR-148a-3p in hucMSC-EVs ameliorates silicotic pulmonary fibrosis was investigated. Hsp90b1 has been demonstrated to be a target of miR-148a-3p and is associated with silica-induced pulmonary fibrosis.[19] The protein-protein interaction (PPI) analysis of Hsp90b1 and the key fibrosis-related genes Fn1, Col1a1, and Acta2 revealed the involvement of Lrp6 and Ctnnb1 in these interactions, with Ctnnb1 playing a central role (Figure 4A). The proteins encoded by Lrp6 and Ctnnb1 are essential in β-catenin signaling, and β-catenin signaling plays an important role in silicosis.[27,28] The protein levels of Grp94 (encoded by Hsp90b1), Lrp6, and β-catenin (encoded by Ctnnb1) were significantly increased in the lung tissues of the silica-exposed mice and were decreased after hucMSC-EVs treatment (Figures 4B-C). Furthermore, these proteins were downregulated in the silica + EVs-virus-miR-148a-3p (+) group compared to the silica + EVs-virus-NC group (Figures 4B-C). Additionally, Grp94 and β-catenin exhibited similar expression localization and consistent change trends in the fibrotic foci of lung tissue, as demonstrated by IHC staining of two consecutive sections that were 5 μm apart from each other within the same sample. This indicates that there might be a certain relationship between them (Figure 4D and Figures S1B-C). These results suggest that β-catenin signaling may be associated with the beneficial effects of miR-148a-3p-mediated hucMSC-EVs on silicotic mouse pulmonary fibrosis.

MiR-148a-3p Could Regulate β-Catenin Signaling in Fibroblasts

To verify if miR-148a-3p influences β-catenin signaling in fibroblasts, miR-148a-3p mimics/mimics NC were transfected into NIH/3T3 cells. The miR-148a-3p level was significantly upregulated, as previously reported.[19] Western blot analysis showed that the Grp94 and β-catenin protein levels were downregulated following miR-148a-3p mimics transfection, as

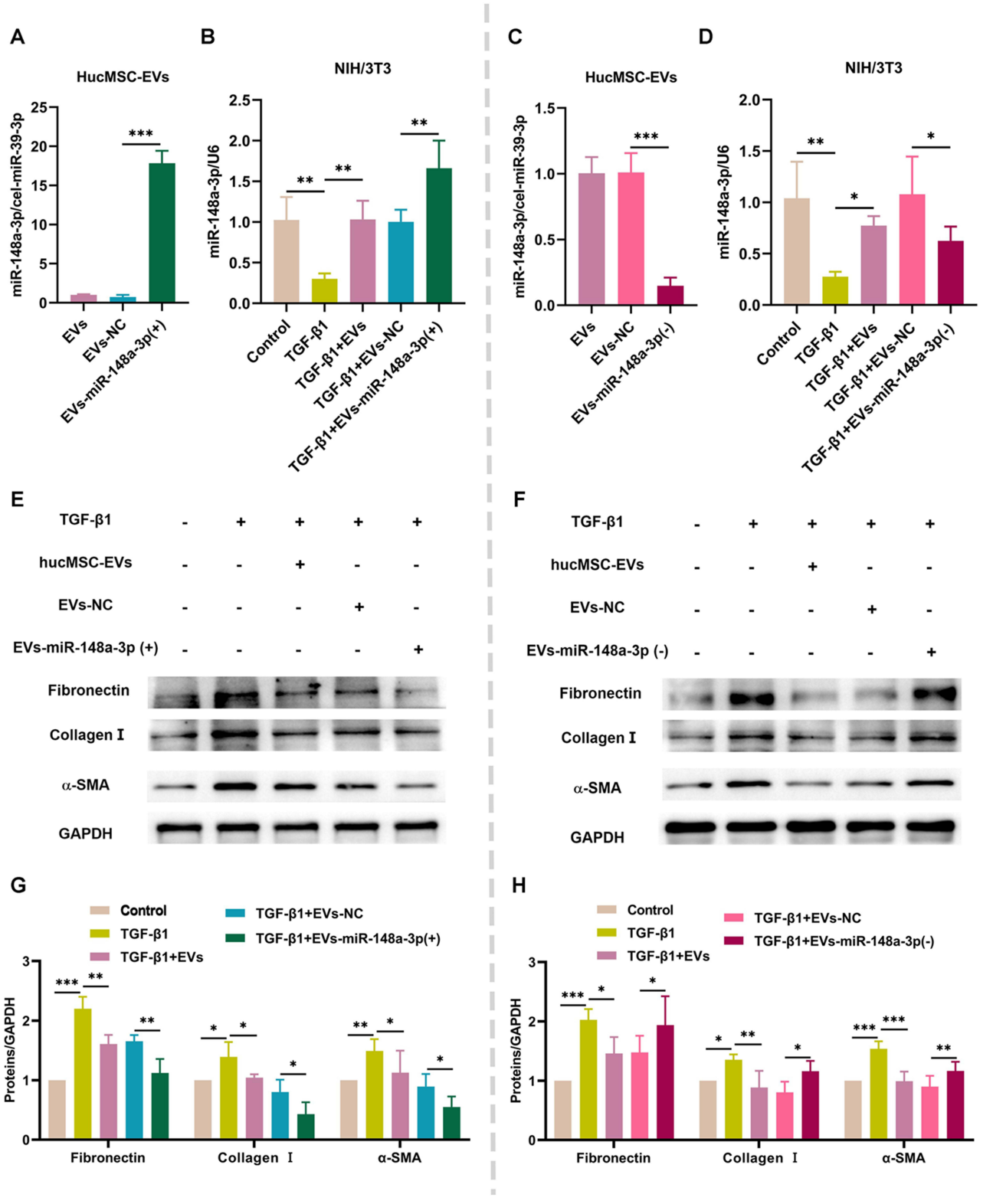

Figure 3 In vitro validation of the function of miR-148a-3p in hucMSC-EVs. (**A** and **C**) The level of miR-148a-3p in hucMSC-EVs isolated from the culture medium of hucMSCs transfected with miR-148a-3p mimics/inhibitor and the corresponding negative control (NC) (n = 3). (**B** and **D**) The expression of miR-148a-3p in NIH/3T3 cells with different inducers (n = 3). (**E - H**) Fibronectin, Collagen I, and α-SMA protein levels in NIH/3T3 cells with different inducers (n = 3–5). *$p < 0.05$, **$p < 0.01$, ***$p < 0.001$ (One-way ANOVA). Data are presented as the means ± SD.

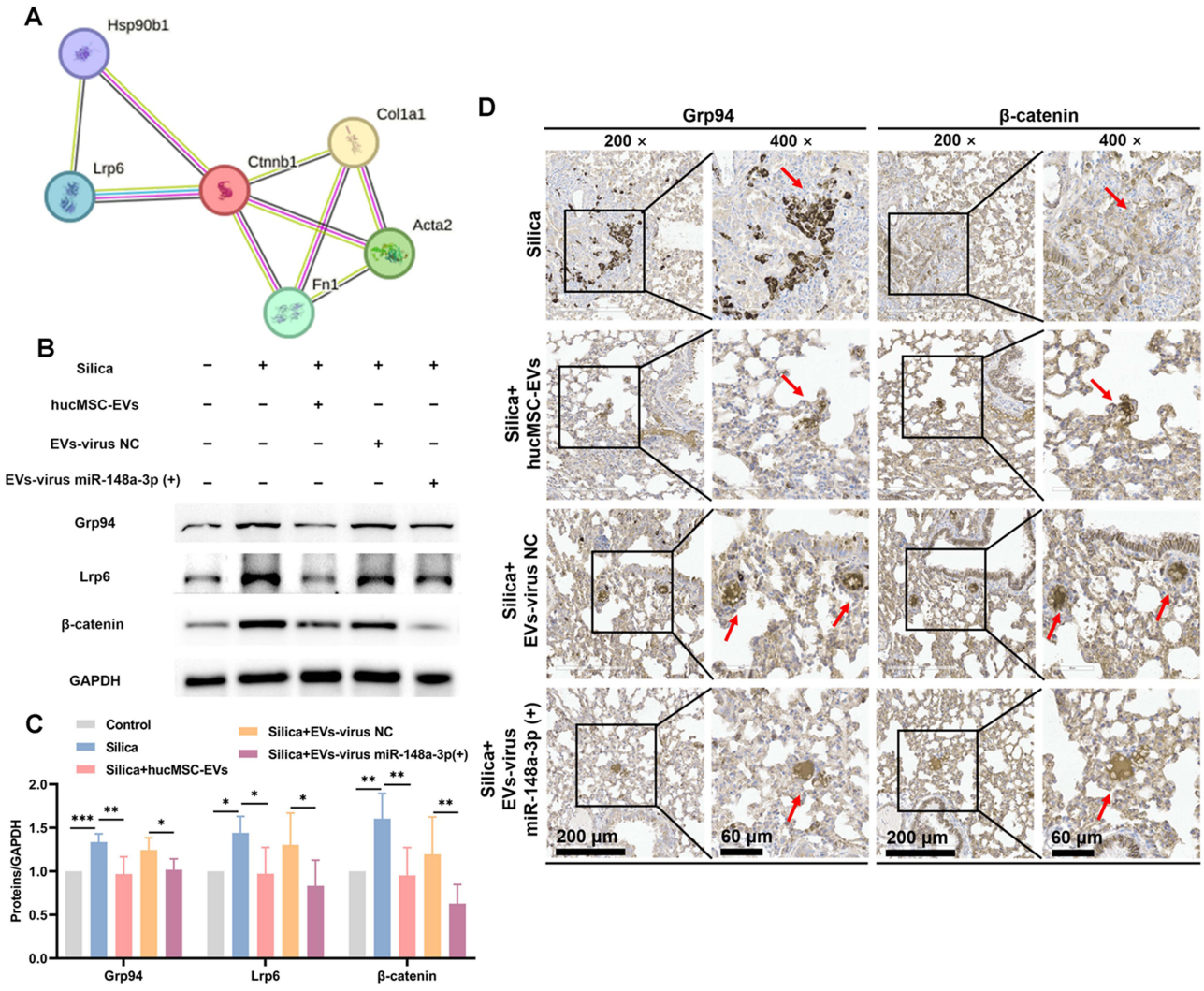

Figure 4 β-catenin signaling is implicated in the anti-fibrotic effect of miR-148a-3p-mediated hucMSC-EVs in silicotic mice pulmonary fibrosis. (**A**) The analysis of PPI involving Hsp90b1 and fibrosis-related genes (Fn1, Col1a1, Acta2). (**B-C**) Grp94, Lrp6, and β-catenin protein levels in the mice lung tissues (n = 4–6). (**D**) IHC staining of Grp94 and β-catenin in lung tissues (200 ×, bar: 200 μm; 400 ×, bar: 60 μm; red arrows: the similar expression localization of Grp94 and β-catenin). *$p < 0.05$, **$p < 0.01$, ***$p < 0.001$ (one-way ANOVA). Data are presented as the means ± SD.

compared to the mimics NC transfection group (Figures 5A-B). Studies have reported that TGF-β1 can induce collagen production in fibroblasts by activating β-catenin signaling.[29] Therefore, changes in β-catenin signaling in miR-148a-3p mimics/mimics NC-transfected NIH/3T3 cells upon TGF-β1 stimulation were assessed. The results showed that the Lrp6 and β-catenin protein levels were markedly increased in the TGF-β1 group but remained low in cells overexpressing miR-148a-3p (Figures 5C-D). The cytoplasmic accumulation of β-catenin and its transposition to the nucleus are considered to characterize the activation of β-catenin signaling.[30] Given that the nuclear translocation of β-catenin is crucial for its action, the subcellular transfer of β-catenin was evaluated via a nuclear/cytoplasmic fractionation experiment. Figures 5E-F demonstrate that TGF-β1 treatment upregulated the β-catenin levels in both the cytoplasm and nucleus, whereas miR-148a-3p mimics treatment suppressed the β-catenin levels in both compartments compared to the TGF-β1 + NC group. Subsequently, immunofluorescence was used to observe β-catenin localization, confirming reduced nuclear translocation in miR-148a-3p mimics- and TGF-β1-treated NIH/3T3 cells (Figure 5G and Figure S1D). These findings indicate that miR-148a-3p attenuated β-catenin signaling activation in fibroblasts.

https://doi.org/10.2147/IJN.S506542

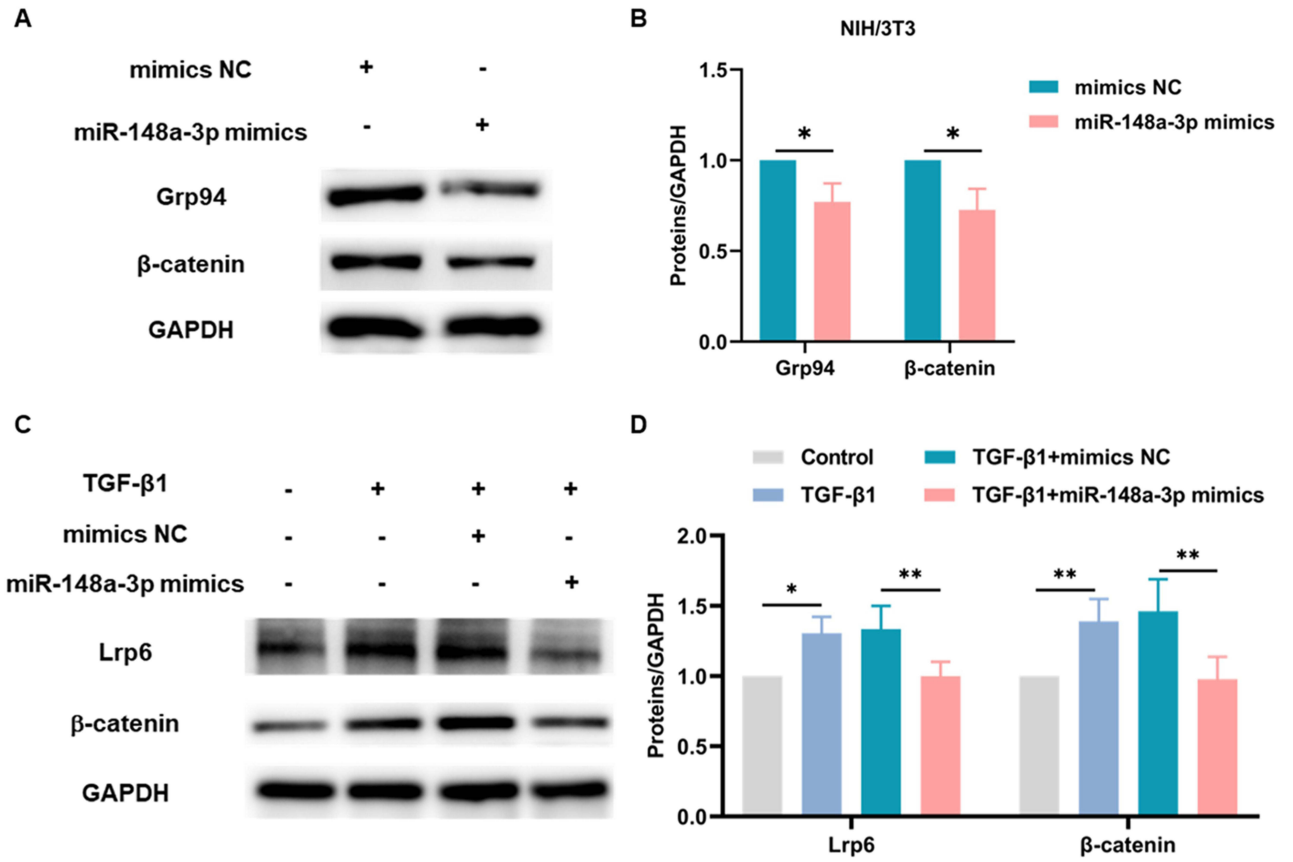

Figure 5 Continued.

Downregulation of Hsp90b1 Restrains TGF-β1-Induced Activation of β-Catenin Signaling in Fibroblasts

The influence of Hsp90b1 on β-catenin signaling was confirmed in TGF-β1-stimulated fibroblasts. The siHsp90b1 was applied to inhibit Hsp90b1 expression prior to establishing the TGF-β1-induced fibroblast collagen hypersecretion model of NIH/3T3 cells. The siHsp90b1 produced a significant reduction in the Grp94 protein level following siHsp90b1 treatment in NIH/3T3 cells.[19] Notably, the Lrp6 and β-catenin levels were found to be decreased in the TGF-β1 + siHsp90b1 group but were at high levels in the TGF-β1 + siNC group (Figures 6A-B). Further, siHsp90b1 effectively blocked cytoplasmic and nuclear accumulation of β-catenin triggered by TGF-β1 (Figures 6C-D). The Western blot results aligned with the immunofluorescence findings, indicating a decrease in β-catenin levels in the NIH/3T3 cells stimulated by TGF-β1 following the siHsp90b1 intervention (Figure 6E and Figure S1E). Thus, these findings indicate that Hsp90b1 downregulation reduced TGF-β1-induced β-catenin signaling activation in fibroblasts.

Discussion

Silicosis remains one of the world's most serious and fatal occupational diseases, with limited treatment options available. Thus, the identification of new treatments for silicosis is of critical importance. This study revealed that hucMSC-EVs administered therapeutically exert antifibrotic effects in an experimental silicotic model. Mechanistically, the results indicated that miR-148a-3p loaded in hucMSC-EVs targets Hsp90b1 to attenuate β-catenin signaling in fibroblasts. These findings offer a potent theoretical basis for the use of hucMSC-EVs in the treatment of silicosis.

Silicosis develops gradually, with early stages characterized by chronic lung inflammatory that drives fibrosis development and nonspecific symptoms, often leading to late diagnosis.[25] Therefore, preclinical studies utilizing silicotic models with established pulmonary fibrosis better reflect the clinical reality of silicosis patients.[8] In this study, we

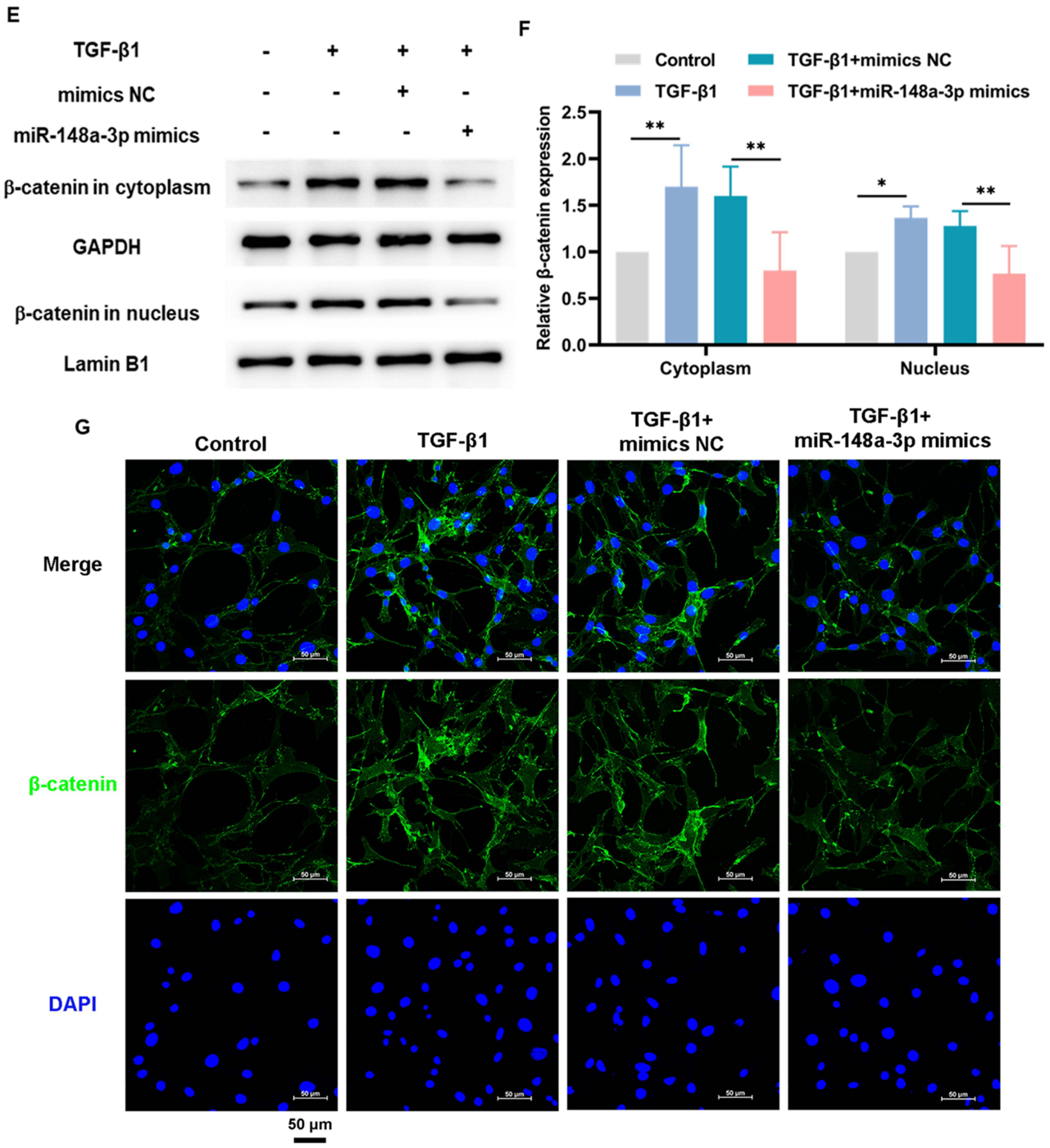

Figure 5 MiR-148a-3p could regulate the β-catenin signaling in fibroblasts. (**A-B**) The protein levels of Grp94 and β-catenin in miR-148a-3p mimics and its negative Control (mimics NC) transfected NIH/3T3 cells (n = 4). (**C-D**) Western blotting analysis of Lrp6 and β-catenin in miR-148a-3p mimics/mimics NC transfected NIH/3T3 cells upon TGF-β1 stimulation (n = 3–8). (**E-F**) The protein levels of cytoplasmic and nuclear β-catenin of NIH/3T3 cells (n = 3–5). (**G**) Immunofluorescence (IF) staining was applied to detect the protein level of β-catenin in NIH/3T3 cells (bar: 50 μm). *$p < 0.05$, **$p < 0.01$ (Student's t-tests was used to compare between two groups and one-way ANOVA was used to compare between multiple groups). Data are presented as the means ± SD.

conducted an in vivo experiment employing a therapeutic administration protocol, unlike the prophylactic administration approach in our earlier studies.[19,26] Lung tissue undergoes fibrosis on day 28 after exposure to silica suspension,[25] so we administered hucMSC-EVs to mice from day 28 to day 56 after silica exposure to evaluate their antifibrotic effects. Results revealed that the lung histopathological changes, the HYP content, and the fibrosis-related proteins levels were

https://doi.org/10.2147/IJN.S506542

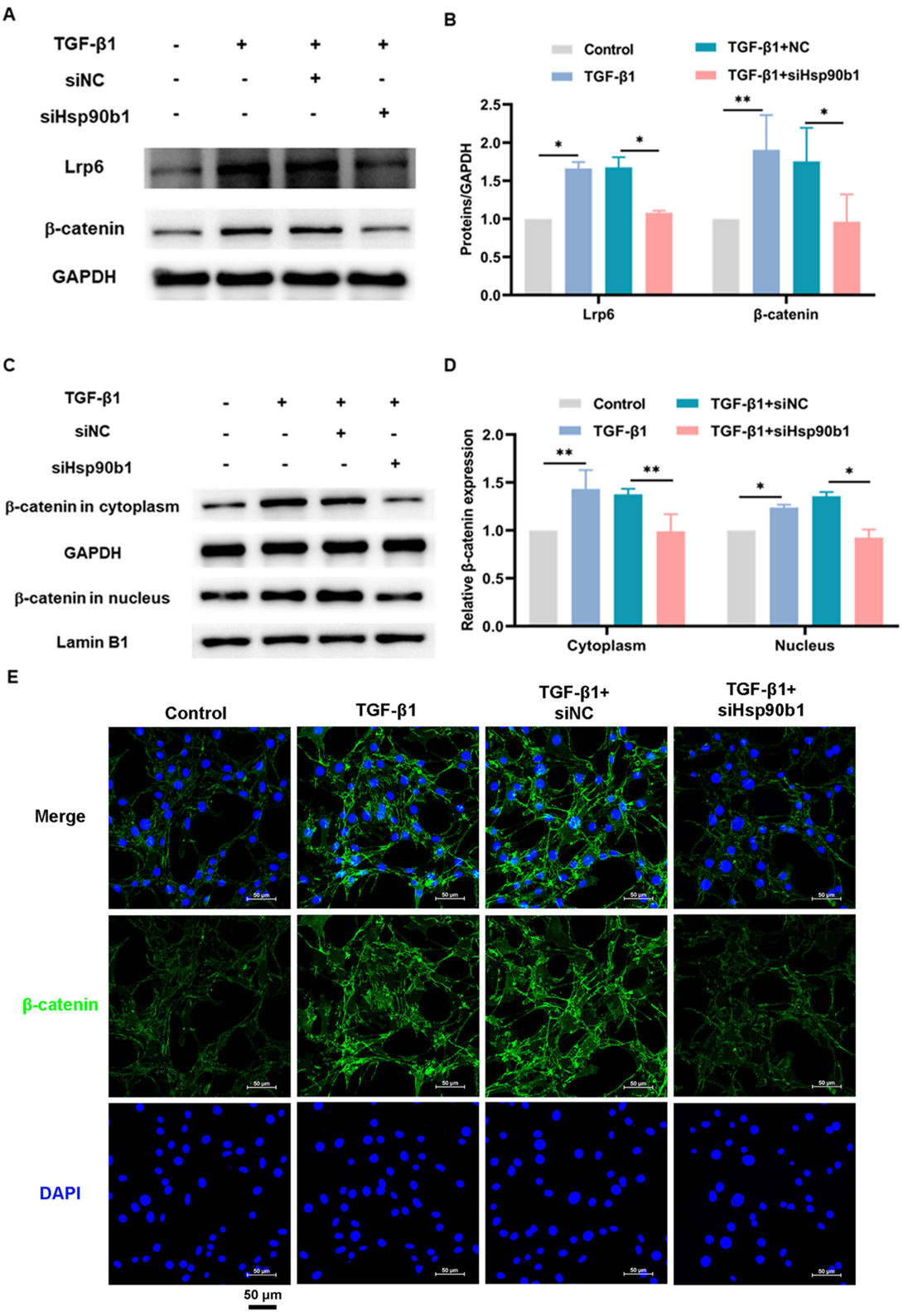

Figure 6 Downregulation of Hsp90b1 restrains TGF-β1-induced activation of β-catenin signaling in fibroblasts. (**A-B**) Lrp6 and β-catenin protein levels in NIH/3T3 cells (n = 3–4). (**C-D**) Protein levels of β-catenin in cytoplasm and nucleus of NIH/3T3 cells (n = 3). (**E**) IF staining was used to detect the protein level of β-catenin in the cytoplasm and nucleus of NIH/3T3 cells (bar: 50 μm). *$p < 0.05$, **$p < 0.01$ (One-way ANOVA). Data are presented as the means ± SD.

attenuated in the silica + hucMSC-EVs group compared with the silica group, suggesting that hucMSC-EVs retain therapeutic efficacy in a silicotic mouse model in which lung fibrosis has already occurred. Other researchers have also explored treatments in silicosis models with established fibrosis, starting interventions on day 14 or day 28 after silica exposure.[8,31,32] These preclinical experimental studies of the effects of drug therapy for silicosis in silicotic animal models that have developed pulmonary fibrosis might offer findings that are more relevant to silicosis patients.

Accumulating evidence indicates that the therapeutic effects of MSC-EVs may be attributed to their loading of miRNAs derived from parental cells.[33–35] Our previous study suggested that high levels of miR-148a-3p loaded in hucMSC-EVs might mediate their capacity to alleviate silica-induced pulmonary fibrosis in mice.[19] The current study further investigated the exact role and potential mechanisms of miR-148a-3p in the antagonistic fibrosis effect of hucMSC-EVs. Initially, lentivirus vectors were applied to generate miR-148a-3p-overexpressed hucMSC-EVs [EVs-virus miR-148a-3p (+)] and EVs-virus NC. Firstly, we assessed the distribution of DiR-labeled EVs-virus miR-148a-3p (+) in mouse lung tissue using an in vivo imaging system (IVIS). The results showed that the fluorescence intensity remained high 96 h after tail vein injection and persisted at 120 h in the isolated mouse lung tissue. This finding is slightly different from that of our earlier in vivo tracking studies in that we detected the fluorescent signals in live mice rather than isolated organs, and the experiment found that the fluorescent signals had largely disappeared in the lung region at 120 h post-tail vein injection.[36,37] Nevertheless, this finding is reasonable given that in vivo fluorescence signal acquisition could be affected by fluorescence signals from the skin, bone, and other non-target organs. In comparison, fluorescence imaging of isolated organs can more accurately reflect the fluorescence distribution in the target organ.[38,39] Therefore, our current detection of fluorescent signals in isolated lung tissue complements the previous in vivo tracking experiment.

In addition, the current results confirmed the previously determined frequency of hucMSC-EVs administration (every 96 hours). This administration regimen was also maintained in the present in vivo animal experiments. Furthermore, the current study has provided rough localization of EVs-virus miR-148a-3p (+) within lung tissue. Immunofluorescence staining analysis of frozen lung tissue sections revealed distinct co-localization of α-SMA, a typical marker for myofibroblasts that emits green fluorescence, with the red fluorescence of PKH26-labeled EVs-virus miR-148a-3p (+). This co-localization might confirm the capacity of EVs-virus miR-148a-3p (+) to bind to myofibroblasts, also known as activated lung fibroblasts, which are the pivotal effector cells in the progression of silicosis. This finding offers novel and powerful insight into the potential mechanisms by which EVs-virus miR-148a-3p (+) might antagonize lung fibrosis. However, it is important to recognize the high heterogeneity of lung fibroblasts.[40] The marker of α-SMA may not be sufficient to recognize the full range of lung fibroblasts, which is a limitation of this study.

The animal experiments revealed that EVs-virus miR-148a-3p (+) more effectively mitigated lung fibrosis compared to the EVs-virus NC-treated group, indicating that the elevated miR-148a-3p content enhanced the anti-fibrotic effect of hucMSC-EVs. This was supported by vitro studies, which indicated that miR-148a-3p in hucMSC-EVs inhibits fibroblast collagen, contributing to their anti-fibrotic activity.[19] Further experiments confirmed that an elevated level of miR-148a-3p in hucMSC-EVs was shown to strengthen the inhibition of fibroblast collagen hypersecretion by hucMSC-EVs, while lower levels weaken it. Together, the combination of in vivo and in vitro assessments highlighted the essential contribution of miR-148a-3p to the ability of hucMSC-EVs to alleviate silica-induced pulmonary fibrosis. These findings also illustrate that miRNAs are vital mediators of the biological functions of MSC-EVs.[14,41]

Further, the results of the current study indicated that the β-catenin signaling pathway is associated with the antagonistic fibrosis effect of miR-148a-3p in hucMSC-EVs. The key molecules in the β-catenin signaling pathway, Lrp6 and Ctnnb1 (encoding the β-catenin protein), were implicated in an interaction network with the miR-148a-3p target gene Hsp90b1 and fibrosis-related genes Fn1, Col1a1, and Acta2. Studies have demonstrated that Hsp90b1 can regulate β-catenin signaling through Lrp6, a coreceptor of β-catenin signaling pathway.[23,24] In this study, the change of Grp94, Lrp6, and β-catenin protein levels in the lung tissues of mice subjected to various treatments was consistent and the upregulated Grp94 and β-catenin were localized similarly within the fibrotic foci of the lung tissues, indicating a potential connection between Grp94 and β-catenin signaling in the silicotic mouse model. We speculated that Grp94 and β-catenin signaling might be involved in the miR-148-3p-mediated inhibitory function of hucMSC-EVs on silicotic pulmonary

fibrosis in mice, as the EVs-virus miR-148a-3p (+) intervention diminished the levels of Grp94, Lrp6, and β-catenin in lung tissues compared to the silica + EVs-virus NC group.

Subsequently, in vitro experiments were performed to test this hypothesis. Since miR-148a-3p has been demonstrated to suppress TGF-β1-induced fibroblast collagen hypersecretion by targeting Hsp90b1,[19] and β-catenin signaling is activated in TGF-β1-treated fibroblasts,[29] the TGF-β1-induced cell model was employed for this analysis. The findings showed the miR-148a-3p mimics and siHsp90b1 treatments effectively reduced β-catenin signaling in TGF-β1-induced hypersecretory phenotype fibroblasts. This indicates that miR-148a-3p can regulate β-catenin signaling by targeting Hsp90b1 to inhibit collagen synthesis and secretion in fibroblasts. Similar findings have been reported in other diseases. In bleomycin-induced pulmonary fibrosis, TGF-β1 could enhance β-catenin signaling thereby leading to the induction of fibroblast differentiation.[42] Further, β-catenin signaling is needed for TGF-β1-induced ECM generation by airway smooth muscle cells.[43] The current research offers new insight into the role of β-catenin signaling in the regulation of collagen synthesis and secretion in fibroblasts, with Hsp90b1 appearing to play a crucial role. Studies have reported that Hsp90b1 can regulate β-catenin signaling by controlling the mature and cell-surface expression of Lrp6.[23,24] However, this was not further verified in the current study as this study focused on the impact on β-catenin, a key determinant of β-catenin signaling. This is a limitation of this study to be addressed in the future.

Conclusion

In summary, the current study demonstrated that hucMSC-EVs retain their antifibrotic properties in silicotic mice when administered in a therapeutic manner. Further, miR-148a-3p was found to be an essential component within hucMSC-EVs, mediating their inhibition of silica-induced pulmonary fibrosis. Finally, miR-148a-3p indicates it regulates the expression of Lrp6 by targeting Hsp90b1, thus deactivating the β-catenin signaling pathway in fibroblasts. These findings offer a substantial new theoretical basis for the use of hucMSC-EVs in the treatment of silicosis.

Abbreviations

α-SMA, alpha-smooth muscle actin; ECM, extracellular matrix; EVs, extracellular vesicles; EVs-virus miR-148a-3p (+)/NC, extracellular vesicles derived from human umbilical cord mesenchymal stem cells transfected with miR-148a-3p-overexpressed/negative control lentivirus vector; EVs-miR-148a-3p (+/-), extracellular vesicles derived from human umbilical cord mesenchymal stem cells transfected with miR-148a-3p mimics/inhibitor; EVs-NC, extracellular vesicles derived from human umbilical cord mesenchymal stem cells transfected with miR-148a-3p mimics NC/ inhibitor NC; HE, hematoxylin and eosin; Hsp90b1, heat shock protein 90 beta family member 1; HucMSCs, human umbilical cord mesenchymal stem cells; HucMSC-EVs, human umbilical cord mesenchymal stem cell-derived extracellular vesicles; HYP, hydroxyproline; IHC, immunohistochemical; Lrp6, low-density lipoprotein receptor-related protein 6; MSCs, mesenchymal stem cells; MSC-EVs, MSC-derived extracellular vesicles; miRNA, microRNA; PPI, protein-protein interaction; siRNA, small interfering RNA; TGF-β1, transforming growth factor-β1.

Data Sharing Statement

Data will be made available on request.

Ethics Approval and Informed Consent

HucMSCs were purchased from NUWACELL Co., Ltd. (Anhui, China), which received approval from the Biomedical Ethics Committee of The First Affiliated Hospital of Anhui Medical University (License Number: PJ2018-01-07). This research adhered to the principles outlined in the Declaration of Helsinki. Written informed consent was obtained from all umbilical cord donors. All animal experiments were approved by the Laboratory Animal Care and Use Committee of Capital Medical University in Beijing, China (AEEI-2022-237) and performed in accordance with the guidelines set forth in the Guide for the Care and Use of Laboratory Animals published by the National Institutes of Health (Eighth Edition).

Author Contributions

All authors made a significant contribution to the work reported, whether that is in the conception, study design, execution, acquisition of data, analysis and interpretation, or in all these areas; took part in drafting, revising or critically reviewing the article; gave final approval of the version to be published; have agreed on the journal to which the article has been submitted; and agree to be accountable for all aspects of the work.

Funding

This research was funded by the National Natural Science Foundation of China under grant 82073522.

Disclosure

Miss Qiyue Jiang reports a patent MiR-148a-3p-loaded extracellular vesicles of human umbilical cord mesenchymal stem cells and their application in the preparation of drugs for silicosis treatment pending to Lin Tian, Qiyue Jiang, Jing Zhao, Chunjie Xu, Zhonghui Zhu, Yan Wang. Dr Zhonghui Zhu reports a patent MiR-148a-3p-loaded extracellular vesicles of human umbilical cord mesenchymal stem cells and their application in the preparation of drugs for silicosis treatment pending to Lin Tian, Qiyue Jiang, Jing Zhao, Chunjie Xu, Zhonghui Zhu, Yan Wang;Professor Lin Tian reports a patent MiR-148a-3p-loaded extracellular vesicles of human umbilical cord mesenchymal stem cells and their application in the preparation of drugs for silicosis treatment pending to Lin Tian, Qiyue Jiang, Jing Zhao, Chunjie Xu, Zhonghui Zhu, Yan Wang. The authors have declared that no competing interest exists.

References

1. Welsh JA, Goberdhan DCI, O'Driscoll L. et al. Minimal information for studies of extracellular vesicles (MISEV2023): from basic to advanced approaches. *J Extracell Vesicles*. 2024;13(2):e12404. doi:10.1002/jev2.12404
2. Rai A, Claridge B, Lozano J, Greening DW. The discovery of extracellular vesicles and their emergence as a next-generation therapy. *Circ Res*. 2024;135(1):198–221. doi:10.1161/CIRCRESAHA.123.323054
3. Abreu SC, Lopes-Pacheco M, Weiss DJ, Rocco PRM. Mesenchymal stromal cell-derived extracellular vesicles in lung diseases: current status and perspectives. *Front Cell Dev Biol*. 2021;9:600711. doi:10.3389/fcell.2021.600711
4. Herrmann IK, Wood MJA, Fuhrmann G. Extracellular vesicles as a next-generation drug delivery platform. *Nat Nanotechnol*. 2021;16(7):748–759. doi:10.1038/s41565-021-00931-2
5. Jia Q, Wang H, Wang Y, et al. Investigation of the mechanism of silica-induced pulmonary fibrosis: the role of lung microbiota dysbiosis and the LPS/TLR4 signaling pathway. *Sci Total Environ*. 2024;912:168948. doi:10.1016/j.scitotenv.2023.168948
6. Sun W, Li Y, Ma D, et al. ALKBH5 promotes lung fibroblast activation and silica-induced pulmonary fibrosis through miR-320a-3p and FOXM1. *Cell mol Biol Lett*. 2022;27(1):26. doi:10.1186/s11658-022-00329-5
7. Krefft S, Wolff J, Rose C. Silicosis: an update and guide for clinicians. *Clin Chest Med*. 2020;41(4):709–722. doi:10.1016/j.ccm.2020.08.012
8. Cao ZJ, Liu Y, Zhang Z, et al. Pirfenidone ameliorates silica-induced lung inflammation and fibrosis in mice by inhibiting the secretion of interleukin-17A. *Acta Pharmacol Sin*. 2022;43(4):908–918. doi:10.1038/s41401-021-00706-4
9. Wollin L, Maillet I, Quesniaux V, Holweg A, Ryffel B. Antifibrotic and anti-inflammatory activity of the tyrosine kinase inhibitor nintedanib in experimental models of lung fibrosis. *J Pharmacol Exp Ther*. 2014;349(2):209–220. doi:10.1124/jpet.113.208223
10. da Silva LH A, Vieira JB, Cabral MR, et al. Development of nintedanib nanosuspension for inhaled treatment of experimental silicosis. *Bioeng Transl Med*. 2023;8(2):e10401. doi:10.1002/btm2.10401
11. Xu C, Zhao J, Li Q, et al. Exosomes derived from three-dimensional cultured human umbilical cord mesenchymal stem cells ameliorate pulmonary fibrosis in a mouse silicosis model. *Stem Cell Res Ther*. 2020;11(1):503. doi:10.1186/s13287-020-02023-9
12. Chen S, Cui G, Peng C, et al. Transplantation of adipose-derived mesenchymal stem cells attenuates pulmonary fibrosis of silicosis via anti-inflammatory and anti-apoptosis effects in rats. *Stem Cell Res Ther*. 2018;9(1):110.
13. Bandeira E, Oliveira H, Silva JD, et al. Therapeutic effects of adipose-tissue-derived mesenchymal stromal cells and their extracellular vesicles in experimental silicosis. *Respir Res*. 2018;19(1):104. doi:10.1186/s12931-018-0802-3
14. Li S, Zhang J, Feng G, et al. The emerging role of extracellular vesicles from mesenchymal stem cells and macrophages in pulmonary fibrosis: insights into miRNA delivery. *Pharmaceuticals*. 2022;15(10)
15. Zhu J, Wang S, Yang D, Xu W, Qian H. Extracellular vesicles: emerging roles, biomarkers and therapeutic strategies in fibrotic diseases. *J Nanobiotechnology*. 2023;21(1):164. doi:10.1186/s12951-023-01921-3
16. Li Y, Sui S, Goel A. Extracellular vesicles associated microRNAs: their biology and clinical significance as biomarkers in gastrointestinal cancers. *Semin Cancer Biol*. 2024;99:5–23. doi:10.1016/j.semcancer.2024.02.001
17. Dhar R, Mukherjee S, Mukerjee N, et al. Interrelation between extracellular vesicles miRNAs with chronic lung diseases. *J Cell Physiol*. 2022;237(11):4021–4036. doi:10.1002/jcp.30867
18. Diener C, Keller A, Meese E. Emerging concepts of miRNA therapeutics: from cells to clinic. *Trends Genet*. 2022;38(6):613–626. doi:10.1016/j.tig.2022.02.006
19. Jiang Q, Zhao J, Jia Q, et al. MiR-148a-3p within HucMSC-derived extracellular vesicles suppresses Hsp90b1 to prevent fibroblast collagen synthesis and secretion in silica-induced pulmonary fibrosis. *Int J mol Sci*. 2023;24(19):14477. doi:10.3390/ijms241914477

20. Villanueva MT. Selective activation of Wnt ameliorates idiopathic pulmonary fibrosis. *Nat Rev Drug Discov*. 2023;22(8):619. doi:10.1038/d41573-023-00116-7
21. Lam AP, Herazo-Maya JD, Sennello JA, et al. Wnt coreceptor Lrp5 is a driver of idiopathic pulmonary fibrosis. *Am J Respir Crit Care Med*. 2014;190(2):185–195. doi:10.1164/rccm.201401-0079OC
22. Weekes MP, Antrobus R, Talbot S, et al. Proteomic plasma membrane profiling reveals an essential role for gp96 in the cell surface expression of LDLR family members, including the LDL receptor and LRP6. *J Proteome Res*. 2012;11(3):1475–1484. doi:10.1021/pr201135e
23. Liu B, Staron M, Hong F, et al. Essential roles of grp94 in gut homeostasis via chaperoning canonical Wnt pathway. *Proc Natl Acad Sci U S A*. 2013;110(17):6877–6882. doi:10.1073/pnas.1302933110
24. Hua Y, White-Gilbertson S, Kellner J, et al. Molecular chaperone gp96 is a novel therapeutic target of multiple myeloma. *Clin Cancer Res*. 2013;19 (22):6242–6251. doi:10.1158/1078-0432.CCR-13-2083
25. Jiang F, Jiang Q, Hou L, et al. Inhibition of macrophage pyroptosis ameliorates silica-induced pulmonary fibrosis. *Ecotoxicol Environ Saf*. 2023;268:115693. doi:10.1016/j.ecoenv.2023.115693
26. Xu C, Hou L, Zhao J, et al. Exosomal let-7i-5p from three-dimensional cultured human umbilical cord mesenchymal stem cells inhibits fibroblast activation in silicosis through targeting TGFBR1. *Ecotoxicol Environ Saf*. 2022;233:113302. doi:10.1016/j.ecoenv.2022.113302
27. Cai Q, Ma J, Wang J, et al. Adenoviral transduction of dickkopf-1 alleviates silica-induced silicosis development in lungs of mice. *Hum Gene Ther*. 2022;33(3–4):155–174. doi:10.1089/hum.2021.008
28. Tian Y, Xia J, Yang G, et al. A2aR inhibits fibrosis and the EMT process in silicosis by regulating Wnt/β-catenin pathway. *Ecotoxicol Environ Saf*. 2023;249:114410. doi:10.1016/j.ecoenv.2022.114410
29. Caraci F, Gili E, Calafiore M, et al. TGF-beta1 targets the GSK-3beta/beta-catenin pathway via ERK activation in the transition of human lung fibroblasts into myofibroblasts. *Pharmacol Res*. 2008;57(4):274–282. doi:10.1016/j.phrs.2008.02.001
30. Clevers H, Nusse R. Wnt/β-catenin signaling and disease. *Cell*. 2012;149(6):1192–1205. doi:10.1016/j.cell.2012.05.012
31. Fan M, Xiao H, Song D, et al. A novel N-arylpyridone compound alleviates the inflammatory and fibrotic reaction of silicosis by inhibiting the ASK1-p38 pathway and regulating macrophage polarization. *Front Pharmacol*. 2022;13:848435. doi:10.3389/fphar.2022.848435
32. Tang Q, Xing C, Li M, Jia Q, Bo C, Zhang Z. Pirfenidone ameliorates pulmonary inflammation and fibrosis in a rat silicosis model by inhibiting macrophage polarization and JAK2/STAT3 signaling pathways. *Ecotoxicol Environ Saf*. 2022;244:114066. doi:10.1016/j.ecoenv.2022.114066
33. Gao L, Qiu F, Cao H, et al. Therapeutic delivery of microRNA-125a-5p oligonucleotides improves recovery from myocardial ischemia/reperfusion injury in mice and swine. *Theranostics*. 2023;13(2):685–703. doi:10.7150/thno.73568
34. Zhang Y, Huang X, Sun T, et al. MicroRNA-19b-3p dysfunction of mesenchymal stem cell-derived exosomes from patients with abdominal aortic aneurysm impairs therapeutic efficacy. *J Nanobiotechnology*. 2023;21(1):135. doi:10.1186/s12951-023-01894-3
35. Oveili E, Vafaei S, Bazavar H, et al. The potential use of mesenchymal stem cells-derived exosomes as microRNAs delivery systems in different diseases. *Cell Commun Signal*. 2023;21(1):20. doi:10.1186/s12964-022-01017-9
36. Hou L, Zhu Z, Jiang F, et al. Human umbilical cord mesenchymal stem cell-derived extracellular vesicles alleviated silica induced lung inflammation and fibrosis in mice via circPWWP2A/miR-223-3p/NLRP3 axis. *Ecotoxicol Environ Saf*. 2023;251:114537. doi:10.1016/j.ecoenv.2023.114537
37. Zhao J, Jiang Q, Xu C, et al. MiR-26a-5p from HucMSC-derived extracellular vesicles inhibits epithelial mesenchymal transition by targeting Adam17 in silica-induced lung fibrosis. *Ecotoxicol Environ Saf*. 2023;257:114950. doi:10.1016/j.ecoenv.2023.114950
38. Yang S, Liu P, Gao T, et al. Every road leads to Rome: therapeutic effect and mechanism of the extracellular vesicles of human embryonic stem cell-derived immune and matrix regulatory cells administered to mouse models of pulmonary fibrosis through different routes. *Stem Cell Res Ther*. 2022;13(1):163. doi:10.1186/s13287-022-02839-7
39. Wiklander OP, Nordin JZ, O'Loughlin A, et al. Extracellular vesicle in vivo biodistribution is determined by cell source, route of administration and targeting. *J Extracell Vesicles*. 2015;4:26316. doi:10.3402/jev.v4.26316
40. Valenzi E, Bulik M, Tabib T, et al. Single-cell analysis reveals fibroblast heterogeneity and myofibroblasts in systemic sclerosis-associated interstitial lung disease. *Ann Rheum Dis*. 2019;78(10):1379–1387. doi:10.1136/annrheumdis-2018-214865
41. Liu H, Chen Y, Yin G, Xie Q. Therapeutic prospects of MicroRNAs carried by mesenchymal stem cells-derived extracellular vesicles in autoimmune diseases. *Life Sci*. 2021;277:119458. doi:10.1016/j.lfs.2021.119458
42. Hu Y, Wang Q, Yu J, et al. Tartrate-resistant acid phosphatase 5 promotes pulmonary fibrosis by modulating β-catenin signaling. *Nat Commun*. 2022;13(1):114. doi:10.1038/s41467-021-27684-9
43. Baarsma HA, Menzen MH, Halayko AJ, Meurs H, Kerstjens HA, Gosens R. β-Catenin signaling is required for TGF-β1-induced extracellular matrix production by airway smooth muscle cells. *Am J Physiol Lung Cell mol Physiol*. 2011;301(6):L956–65. doi:10.1152/ajplung.00123.2011